

Multicaloric effect in synergic magnetostructural phase transformation Ni-Mn-Ga-In alloys

Hanyang Qian^{1,2,*}, Jianping Guo^{1,3,*}, Zhiyang Wei^{1,2,†} and Jian Liu^{4,‡}

¹CAS Key Laboratory of Magnetic Materials and Devices, Ningbo Institute of Materials Technology and Engineering, Chinese Academy of Sciences, Ningbo 315201, China

²University of Chinese Academy of Sciences, 19 A Yuquan Road, Shijingshan District, Beijing 100049, China

³Department of Physics, Technical University of Munich, 85748 Garching bei Munich, Germany

⁴School of Materials Science and Engineering, Shanghai University, Shanghai 200444, China



(Received 15 November 2021; accepted 28 March 2022; published 2 May 2022)

Multicaloric effect refers to a thermal response of materials driven by more than one external field. In this work, using a self-designed multicaloric effect characterization setup, we directly measured the adiabatic temperature change (ΔT_{ad}) under uniaxial stress and magnetic field for a spin-lattice synergic coupled system of Ni-Mn-Ga-In. Both stress and magnetic field favor the martensitic transformation. A large ΔT_{ad} of -6.7 K was achieved in the $\text{Ni}_{57}\text{Mn}_{18}\text{Ga}_{21.45}\text{In}_{3.55}$ alloy when simultaneously applying a moderate dual-external-field (uniaxial stress of 95 MPa and magnetic field of 2 T). Such a multicaloric ΔT_{ad} is 72% higher than the single elastocaloric cooling, which is ascribed to the larger transformation volume fractions obtained under dual fields. Additionally, benefiting from the reduction in critical stress by a bias magnetic field, $\text{Ni}_{57}\text{Mn}_{18}\text{Ga}_{21.45}\text{In}_{3.55}$ exhibits a good fatigue resistance with a relatively stable ΔT_{ad} of -5.7 K upon dual-field cycles of about 600 times. Our experimental results reveal that the multicaloric strategy based on the synergic magnetostructural transformation is feasible and promising for solid-state cooling under relatively lower driven fields.

DOI: [10.1103/PhysRevMaterials.6.054401](https://doi.org/10.1103/PhysRevMaterials.6.054401)

I. INTRODUCTION

Due to energy scarcity and global warming, solid-state refrigeration based on magnetocaloric, elastocaloric, and electrocaloric effects has been considered as a promising alternative candidate for conventional vapor compression cooling systems [1–5]. Recently, multicaloric effect driven by more than one external field has been drawing increasing interest and become the focus in the solid-state cooling society [6–11]. Multicaloric effect based on the coupling of the magnetocaloric and elastocaloric effects is beneficial to broaden the operating temperature range, to reduce first-order phase transformation hysteresis, as well as to decrease driving fields for the compact devices [12–15]. The prerequisite for realizing the magnetoelastic cooling system is that the refrigerant materials should hold a strong spin-lattice interaction characteristic. Ni-Mn-based Heusler alloys are typical magnetoelastic coupling materials [16,17], but owing to intrinsic brittleness they are prone to crack on phase transformation, especially under the high magnetic or stress external field. On the other hand, it is hard to complete phase transformation under the low driving field, therefore resulting in a small caloric effect [18–20]. So, the question arises of whether one can achieve a high phase transforming volume and large caloric response by applying relatively low fields. It has been reported that the combination of magnetic field and stress is capable

to manipulate the magnetostructural transformation behaviors for Ni-Mn-based Heusler alloys [12,17,21,22]. However, for the kind of Ni-Mn-In/Sn/Sb alloys, high-temperature ferromagnetic (FM) austenite transforms to low-temperature paramagnetic (PM) or antiferromagnetic (AFM) martensite. The application of extra magnetic field favors the FM austenite and results in an increase in stress to trigger the martensite phase transformation [12,21,23]. Moreover, the total entropy change becomes weakened due to the contrary contribution of magnetic entropy change and lattice entropy change [24,25]. Here, such spin-lattice competitive transformation is termed nonsynergic magnetostructural transformation.

In contrast, for synergic magnetostructural transformation, materials transform from high-temperature PM austenite to low-temperature FM martensite. As schematically demonstrated in Fig. 1, both magnetic field and stress promote the martensite formation and bring about a positive contribution of magnetism and lattice to the total entropy change. Thus, for such synergic multicaloric materials, the critical field is expected to be reduced. To our knowledge, few multicaloric effects based on synergic type transformation have been reported. For instance, Castillo-Villa *et al.* found that in $\text{Ni}_{50.5}\text{Mn}_{21.7}\text{Ga}_{24.7}\text{Co}_{3.1}$, the magnetic entropy change of $2.5 \text{ J kg}^{-1} \text{ K}^{-1}$ can be enhanced to $3 \text{ J kg}^{-1} \text{ K}^{-1}$ on simultaneously applying 10 MPa stress and 1 T magnetic field [26]. It should be noted that due to its weak magnetoelastic coupling strength, the multicaloric effect in $\text{Ni}_{50.5}\text{Mn}_{21.7}\text{Ga}_{24.7}\text{Co}_{3.1}$ is not very significant.

In this work, we report a synergic spin-lattice transformation system of Ni-Mn-Ga-In alloys exhibiting a strong magnetoelastic coupling. Self-designed multicaloric effect

*These authors contributed equally to this work.

†weizhiyang@nimte.ac.cn

‡liujian@nimte.ac.cn

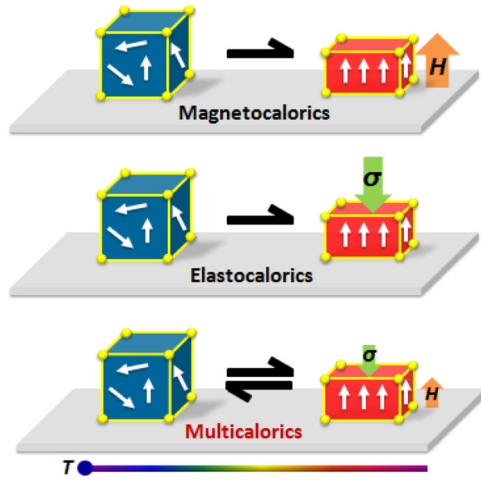


FIG. 1. A schematic illustrating the characteristics of multicaloric effect based on synergic magnetostructural transformation. Compared with the single-caloric effect, the dual-field application approach enables to reduce the magnitude of applied magnetic field and uniaxial stress.

characterization equipment was used to directly figure out the multiple-field induced adiabatic temperature change (ΔT_{ad}). As a result of the simultaneous application of uniaxial stress and magnetic field, distinct lowered critical fields, larger transformation volume fraction, and enhanced caloric effect have been obtained in Ni-Mn-Ga-In alloys.

II. EXPERIMENTAL METHODS

A series of $\text{Ni}_{57}\text{Mn}_{18}\text{Ga}_{25-x}\text{In}_x$ ($x = 3.4, 3.55, 3.7, 3.82, 3.9, 4.0, 4.3$) alloys was synthesized by using arc melting in Ar atmosphere. To compensate for the evaporation of Mn during melting, 0.2% extra Mn was added. The ingots were then cast into 7-mm-diameter rods, and to improve the fatigue resistance of the materials, the rods were directionally solidified by the liquid-metal cooling method to form crystallites with a [001] preferred orientation, which was determined by x-ray diffraction. The crystal growth rate was set to be $150 \mu\text{m s}^{-1}$ at 1523 K. A rectangular specimen with a dimension of $4 \times 4 \times 8 \text{ mm}^3$ for compressive tests were cut from the directionally solidified rods and subsequently annealed at 1148 K for 48 h in Ar atmosphere followed by rapid quenching in ice water. A differential scanning calorimeter (DSC 214, NETZSCH) was used to determine phase transformation temperatures and specific heat. A superconducting quantum interference device (SQUID) magnetometer (MPMS, Quantum Design Inc) was used to measure magnetic properties.

Stress-strain curves and ΔT_{ad} under simultaneous magnetic field and uniaxial stress were directly characterized by using a bespoke multicaloric effect characterization equipment, as schematically shown in Fig. 2. This setup mainly consists of a purpose-built universal testing machine and a superconducting magnet. The universal testing machine can provide a maximum force of 20 kN where the stress is measured by a spoke-structure pressure sensor (PSD-5t-SJTT, CELTRON) and a superconducting magnetic system (Cryogenic Ltd.) with

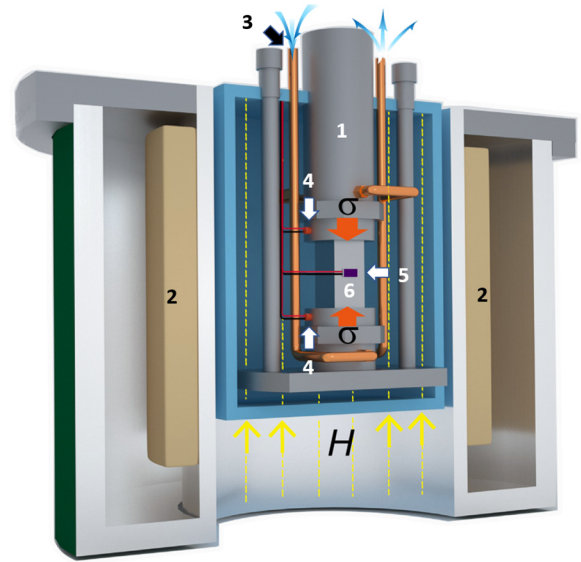


FIG. 2. Sketch of multicaloric effect characterization equipment. (1) Loading heads of universal testing machine. (2) Superconducting magnet. (3) Liquid nitrogen circulation tube. (4) Alumina ceramic heating rods. (5) Cryogenic temperature sensor. (6) Specimen with a rectangle shape.

a maximum magnetic field up to 5 T. The operating temperature can be adjusted continuously in the range 100–350 K through the liquid nitrogen circulation system and alumina ceramic heating rods that are connected with the loading heads. The specimen contacts the loading heads directly to ensure the heat flow between the sample and the loading head for more precise temperature control. A cryogenic temperature sensor (DT-670, LakeShore) is attached to the specimen to monitor its temperature. A customized extensometer (Epsilon) being able to work in a magnetic field is used to record strain. All these components are integrated in a vacuum chamber which is connected to mechanical and molecular pumps to ensure adiabatic environment during the test to improve the accuracy of the ΔT_{ad} measurement. In compression experiments, the loading and unloading rates were set to be 2 and 10 mm min^{-1} , respectively.

III. RESULTS AND DISCUSSION

A. Synergic magnetostructural transformation behavior

DSC curves upon heating and cooling for $\text{Ni}_{57}\text{Mn}_{18}\text{Ga}_{25-x}\text{In}_x$ ($x = 3.4, 3.55, 3.7, 3.82, 3.9, 4.0, 4.3$) alloys are shown in Fig. 3(a). The martensitic transformation temperature (T_{tr}^{DSC}) is assessed by $T_{tr}^{DSC} = (A_s + A_f + M_s + M_f)/4$, where A_s , A_f , M_s , and M_f are the starting and finishing temperature for austenite and martensite, respectively and determined by tangent method from the DSC curves. T_{tr}^{DSC} decreases with the increase of the In content [Fig. 3(b)]. Since the transformation temperature is sensitive to the In concentration, a slight compositional fluctuation may cause a non-negligible shift in transformation temperature and thus a scatter behavior of transformation temperature from the linear tendency was observed. Nevertheless, a linear relationship

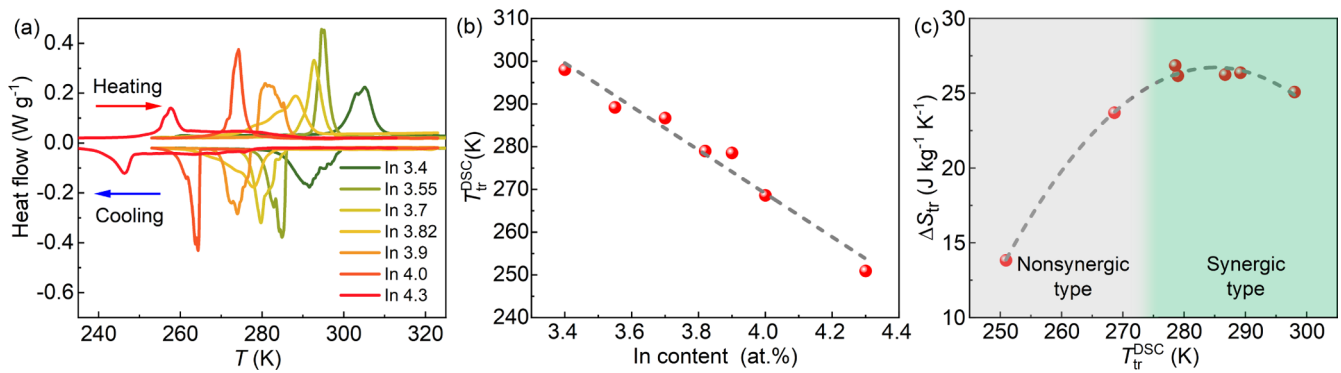


FIG. 3. (a) DSC curves for Ni₅₇Mn₁₈Ga_{25-x}In_x upon heating and cooling. (b) T_{tr}^{DSC} as a function of the In content. (c) ΔS_{tr} as a function of T_{tr}^{DSC} .

between transformation temperature and In content is apparent. The transformation entropy change ΔS_{tr} is taken as the average value of entropy change upon heating and cooling. The entropy change upon heating and cooling are calculated as $2\Delta H_h/(A_s + A_f)$, $2\Delta H_c/(M_s + M_f)$, where ΔH_h and ΔH_c are the transformation enthalpy change and respectively determined from the peak area upon heating and cooling DSC curves. As shown in Fig. 3(c), ΔS_{tr} first increases till $T_{tr} = 278$ K ($x = 3.9$) and then keeps almost constant ~ 25 J kg⁻¹ K⁻¹. This tendency is related to the magnetostructural coupling effect as discussed below.

Figures 4(a)–4(g) show the thermomagnetic (M - T) curves recorded upon heating and cooling for Ni₅₇Mn₁₈Ga_{25-x}In_x alloys measured at various magnetic fields from 0.05 to 5 T. Alloys with higher In content ($x \geq 3.9$) exhibit a separated transformation behavior: upon cooling, they ferromagnetically order at Curie temperatures (T_C) first, and then undergo the martensitic transformation accompanied with a magnetization drop under low fields. Here the T_{tr}^{mag} is evaluated by $T_{tr}^{mag} = (A_s + A_f + M_s + M_f)/4$, where A_s , A_f , M_s , and M_f are determined by tangent method from the M - T curves. As the In content decreases, T_{tr}^{mag} increases while T_C decreases slightly, which is in agreement with previous reports [16,27]. The In content dependencies of T_{tr}^{mag} and T_C result in a synergic coupled magnetostructural transformation and an increased ΔS_{tr} when $x < 3.9$. The magnetostructural transformation is shifted towards higher temperatures due to the Zeeman energy difference between martensite and austenite. dT_{tr}^{mag}/dH refers to the sensitivity of the magnetostructural transformation temperature affected by external magnetic field. In first-order martensite transformation, dT_{tr}^{mag}/dH is supposed to be relevant to the strength of magnetoelastic coupling and caloric effect. This key parameter becomes higher in alloys with spin-lattice coupled transformation ($x < 3.9$), as seen in (h). It was found that Ni₅₇Mn₁₈Ga_{21.45}In_{3.55} exhibits both magnetoelastic coupling effect and large entropy change among Ni₅₇Mn₁₈Ga_{25-x}In_x ($x = 3.4, 3.55, 3.7, 3.82, 3.9, 4.0, 4.3$) alloys. Therefore, we selected Ni₅₇Mn₁₈Ga_{21.45}In_{3.55} for this study.

Ni₅₇Mn₁₈Ga_{21.45}In_{3.55} has $T_{tr}^{mag} = 294$ K under 0.05 T and a dT_{tr}^{mag}/dH of 0.92 K T⁻¹. dT_{tr}^{mag}/dH with a positive value of 0.92 K T⁻¹ indicates a synergic-type magnetostructural transformation. The magnetocaloric entropy changes ΔS_M was

calculated using the Maxwell thermodynamic relationship, $S_M(T, H) = \int_0^H (\frac{dM}{dT})_H dH$, as plotted in Fig. 4(i). The values of ΔS_M are 13.4 J kg⁻¹ K⁻¹ in a magnetic field change of 2 T and 23 J kg⁻¹ K⁻¹ in 5 T.

B. Direct measurement of multicaloric effect

The martensitic transformation behavior and caloric response under simultaneous application of uniaxial stress and magnetic field were investigated for Ni₅₇Mn₁₈Ga_{21.45}In_{3.55}. Figure 5(a) illustrates the stress-strain curves corresponding to isothermal loading and adiabatic unloading under various magnetic fields from 0 to 4 T at 310 K. The maximum applied stress was set as 95 MPa for each loading/unloading cycle. For each curve, a superelastic plateau is observed, reflecting a stress-induced martensitic transformation. The increased slope of stress-strain curves after the plateau indicates an elastic deformation of martensite, suggesting that the transformation is nearly complete under 95 MPa and magnetic field above 1 T. It is evident that the critical stress σ_{cr} to induce martensitic transformation decreases as magnetic field increases with an almost linear relation, as shown in Fig. 5(b). The value of σ_{cr} is 79 MPa in absence of a bias magnetic field, while it is reduced to 62 MPa in a bias magnetic field of 4 T. The magnetic field dependence of critical stress $d\sigma_{cr}/dH$, is estimated to be -4.1 MPa T⁻¹. In addition, the transformation strain ε_{tr} was increased with magnetic field from 1.4% (0 T) to 2.1% (2 T), and then to 2.5% (4 T). The reduced σ_{cr} and increased ε_{tr} by the application of additional magnetic field are associated with significant synergic type transformation in the present Ni-Mn-Ga-In, which is in strong contrast to the nonsynergic-type materials, such as Ni-Co-Mn-In [28].

The superelastic cooling effect with a varying magnetic field is presented in Fig. 5(c). $\Delta T_{ad} = -3.9$ K is observed upon rapid unloading from 95 MPa stress without the assistance of a magnetic field, whereas ΔT_{ad} was substantially enhanced to -6.7 and -7.3 K as the magnetic field increased to 2 and 4 T, respectively. Because of a similar dependence of ΔT_{ad} and ε_{tr} on the magnetic field [see Fig. 5(d)], it suggests that the enhanced ΔT_{ad} is closely related to a larger transformation volume fraction by dual fields. It is worthwhile to note that $|\Delta T_{ad}|$ with the value 7.3 K under 95 MPa and 4 T is much smaller than the theoretical value of 17.4 and 20.0 K which are estimated by $\Delta T_{ad} = \Delta S_{tr} \times T_{tr}/C_p$

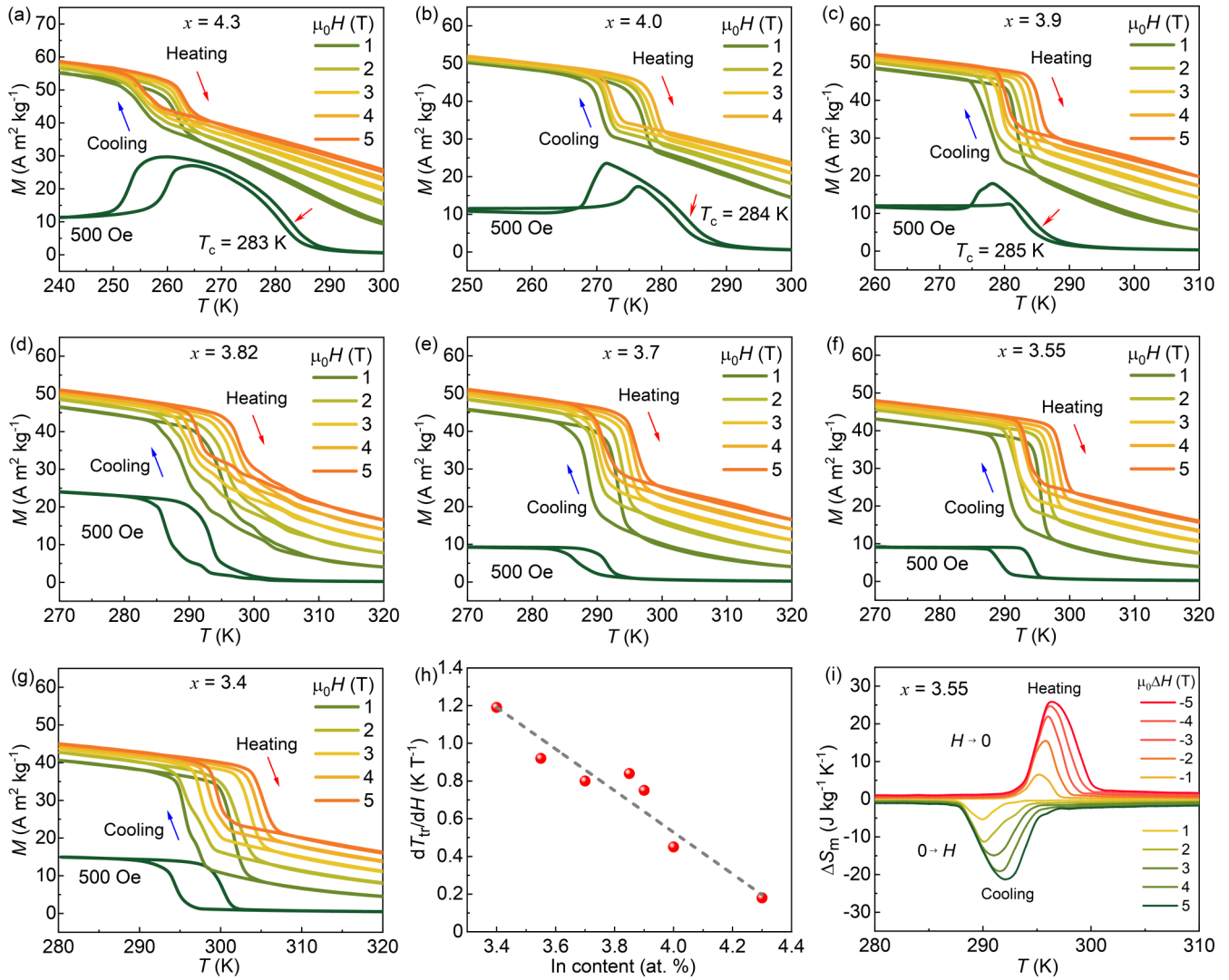


FIG. 4. Thermomagnetic curves for $\text{Ni}_{57}\text{Mn}_{18}\text{Ga}_{25-x}\text{In}_x$ alloys upon heating and cooling are presented in (a)–(g). (h) The $dT_{\text{tr}}^{\text{mag}}/dH$ as a function of the In content. (i) Magnetic entropy changes as a function of temperature under different magnetic fields for $x = 3.55$.

from magnetization and heat capacity measurement, respectively. Such a deviation may be ascribed to the following reasons. First, the temperature control in this work is realized by the heat exchange between the loading heads and the sample, so the sample directly contacts the loading heads. Such heat exchange degrades the adiabatic condition upon stress loading or unloading. Second, the unloading rate is set as 10 mm min^{-1} ($\sim 0.02 \text{ s}^{-1}$) which is insufficient to achieve an adiabatic condition. Both factors result in the difference between experimental and theoretical ΔT_{ad} . Another aspect influenced by the extra magnetic field is the large stress hysteresis. Though the transformation hysteresis increases in higher magnetic fields, there is no residual stress from stress-strain loops [see Fig. 5(a)], which indicates the good phase transformation reversibility.

Next, we take the coefficient of performance (COP_{mat}) to assess the multicaloric refrigeration efficiency. COP_{mat} refers to the coefficient of performance based on material properties following the ideal cycle and it is a material performance metric to compare different elastocaloric materials. Different from Brayton and Stirling cycles [29], the thermodynamic cycle

adopted in our work consists of an isothermal loading and an adiabatic unloading under magnetic field. The corresponding COP_{mat} is calculated based on the following equation [30]:

$$COP_{\text{mat}} = \frac{T_c \Delta S_{\text{mul}} - \frac{\Delta E_{\text{irre}} + \Delta T_{\text{ad}} \Delta S_{\text{mul}}}{2}}{\Delta E_{\text{irre}} + (T_h - T_c + \frac{\Delta T_{\text{ad}}}{2}) \Delta S_{\text{mul}}}, \quad (1)$$

where T_c and T_h are the cold and hot temperatures in heat exchangers, respectively. ΔS_{mul} , the entropy change response to multiple fields, is estimated by $\Delta S_{\text{mul}} = q/T_c$, where q is the absorbed heat calculated by $q = C_p \times \Delta T_{\text{ad}}$. ΔE_{irre} is the irreversibility of the phase transformation process, as determined by

$$\Delta E_{\text{irre}} = \oint \frac{\sigma_{\text{cr}} d\varepsilon_{\text{tr}}}{\rho} - 1/2 \Delta T_{\text{ad}} \Delta S_{\text{mul}}. \quad (2)$$

Although the magnetic field enhances the caloric effect, the resultant larger hysteresis requires more work to accomplish the cycle in the denominator of Eq. (1) and leads to the decrease in COP_{mat} from 18.2 to 13.3 when external magnetic field increases from 0 to 4 T. The data of COP_{mat}

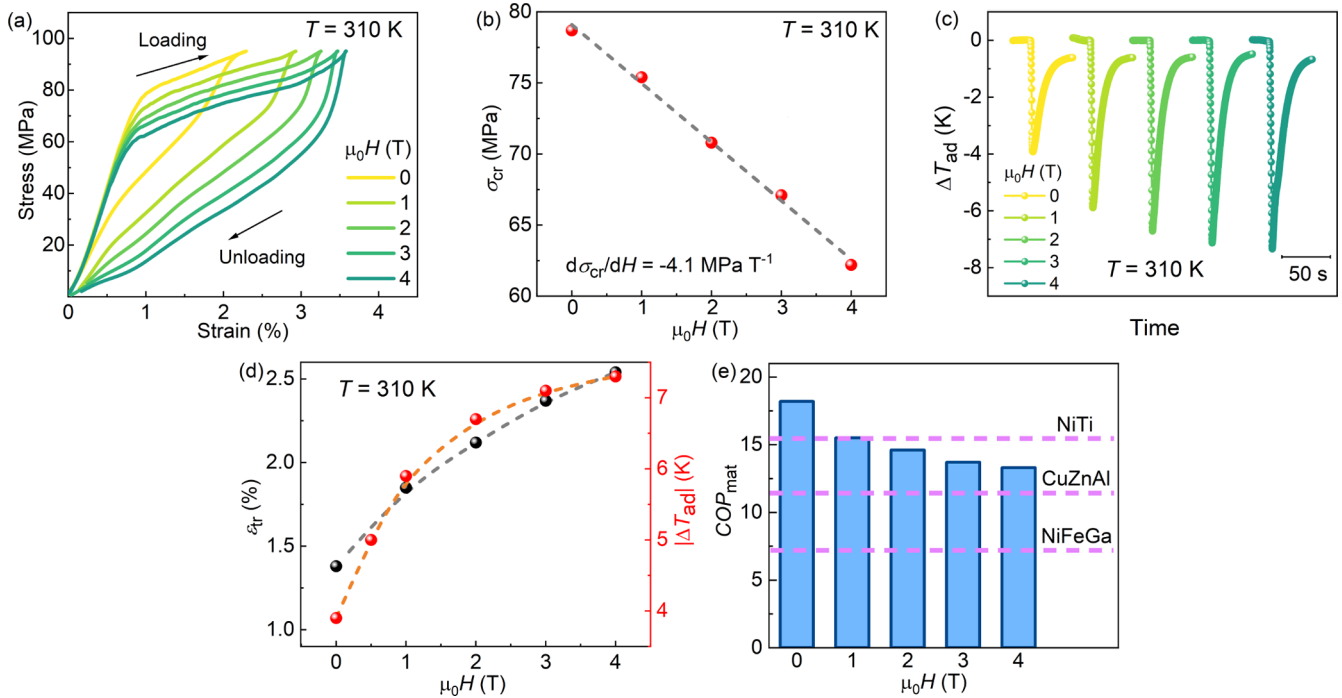


FIG. 5. (a) Stress-strain curves upon loading and unloading measured in magnetic fields from 0 to 4 T at 310 K. (b) Critical stress σ_{cr} as a function of magnetic field. (c) ΔT_{ad} obtained during unloading in various magnetic fields corresponding to (a). (d) Magnetic field dependence of ϵ_{tr} and ΔT_{ad} . (e) COP_{mat} as a function of magnetic field.

for $Ni_{57}Mn_{18}Ga_{21.45}In_{3.55}$ is in comparison with other typical elastocaloric alloys in Fig. 5(e). It can be seen that the multicaloric COP_{mat} is 14.6 in 2 T magnetic field for $Ni_{57}Mn_{18}Ga_{21.45}In_{3.55}$, which is comparable to that for Ni-Ti ($COP_{mat} = 15.5$), while higher than Cu-Zn-Al ($COP_{mat} = 11.4$) and Ni-Fe-Ga ($COP_{mat} = 7.2$) alloys [30].

For our alloy, the multicaloric effects is not constricted at a certain temperature but could be achieved within a temperature window. The isothermal stress-strain curves under various magnetic fields at different temperatures 302, 305, and 310 K were recorded for $Ni_{57}Mn_{18}Ga_{21.45}In_{3.55}$, which enables us to establish σ_{cr} as a function of both magnetic field and temperature, as presented in Fig. 6(a). For a certain temperature within the temperature range, lower σ_{cr} can be obtained with the assistance of external magnetic field. A low driven stress is desired because the fatigue resistance can be greatly improved, especially for brittle Ni-Mn-based Heusler alloys. Moreover, σ_{cr} can be further lowered when temperature decreases. For instance, at 302 K, σ_{cr} is as low as 20 MPa when applying a magnetic field of 5 T. However, at this temperature, the irreversibility of transformation resulting from the appearance of the temporary residual strain must be taken into consideration [31].

As presented in Fig. 3, the magnetic field brings the T_{tr} higher and closer to the testing temperature, thus a larger transformation volume fraction and a larger ΔT_{ad} can be achieved under a certain stress. It seems that lowering ambient temperature is equivalent to the strategy of applying a magnetic field. However, the working temperature in practical application is certain, and it is not possible to lower the ambient temperature to satisfy the materials' properties.

Here we demonstrated a strategy that, by applying an external magnetic field to broaden the working temperature range, provides a more flexible routine than lowering the working temperature. Thus, upon stress unloading, applying an external magnetic field to broaden the working temperature range provides a strategy to make the best of the materials. Additionally, from Fig. 6(a), $dT_{tr}/d\sigma$ is calculated to be 0.21 K MPa^{-1} and exhibits a weak dependency on magnetic field. Considering the theoretical adiabatic temperature change -20.0 K which is estimated from DSC measurement, it also confirms that a uniaxial stress with a value of around 95 MPa is sufficient to drive an almost complete transformation.

The response of σ_{cr} to the external magnetic field is described by the magnetostress, which is defined as the change in critical stress to trigger phase transformation with and without an external magnetic field [32]. The magnetostress as a function of magnetic field for $Ni_{57}Mn_{18}Ga_{21.45}In_{3.55}$, in comparison with two typical Heusler systems, Ni-Mn-Ga (relevant data from Ni_2MnGa [32]) and Ni-Co-Mn-In (reference data from $Ni_{45}Co_5Mn_{36.5}In_{13.5}$ [33]), is plotted in Fig. 6(b). The mechanism of the magnetostress for these materials are rather different as illustrated in Fig. 6(c): (i) In Ni-Mn-Ga alloys, the magnetostress is relevant to the magnetic-field-favored martensite variants reorientation, which greatly relies on magnetocrystalline anisotropy [32]. Since the magnetostress is limited by anisotropy energy, even if a large magnetic field is applied, the value of output stress in Ni-Mn-Ga is restricted. (ii) Magnetostress in Ni-Co-Mn-In arises from the martensitic transformation and the Zeeman energy, because of the magnetization difference between AFM martensite and FM austenite [34]. The external magnetic field stabilizes the FM

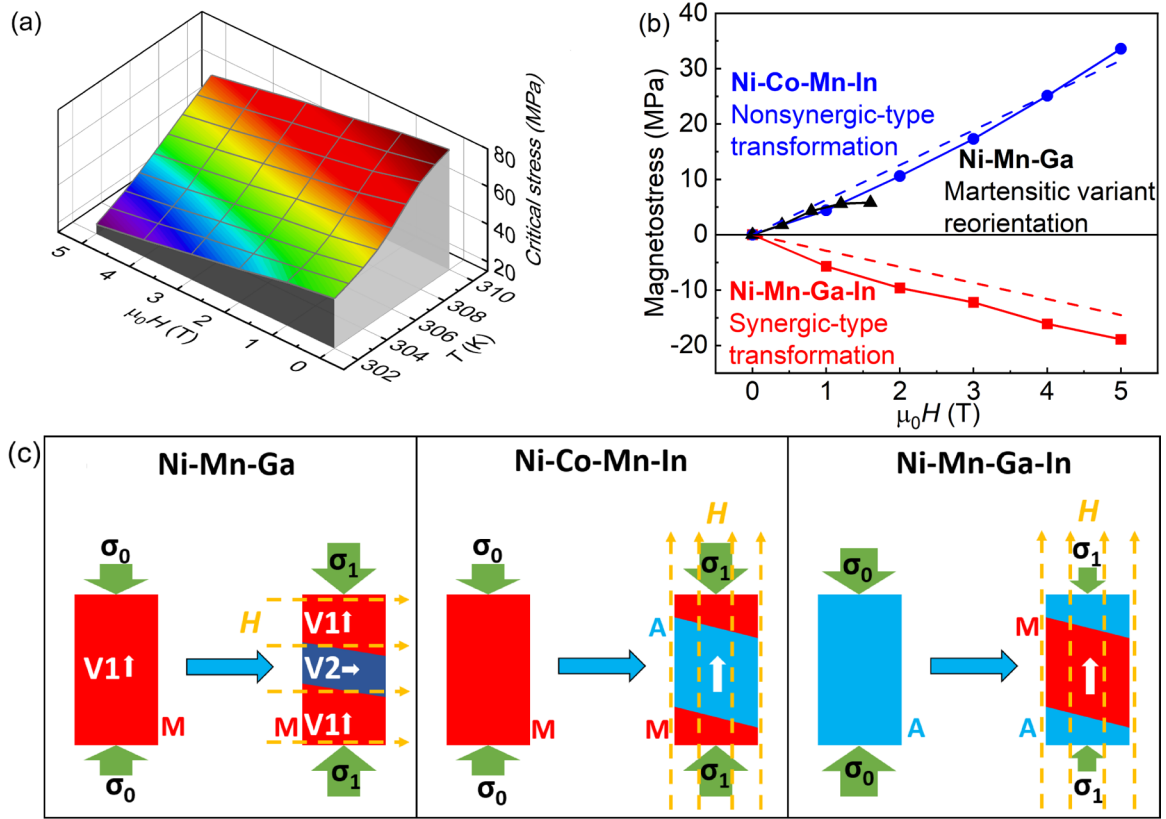


FIG. 6. (a) Critical stress as a function of and temperature and magnetic field for $\text{Ni}_{57}\text{Mn}_{18}\text{Ga}_{21.45}\text{In}_{3.55}$. (b) Magnetostress as a function of magnetic field for $\text{Ni}_{57}\text{Mn}_{18}\text{Ga}_{21.45}\text{In}_{3.55}$ (310 K), $\text{Ni}_{45}\text{Co}_5\text{Mn}_{36.5}\text{In}_{13.5}$, and Ni_2MnGa (experimental and calculated results are marked by solid and dash line, respectively). (c) Schematics of magnetostress for the three alloys, where V1, V2 represent martensite variant 1 and martensite variant 2, and A and M refer to austenite and martensite, respectively. White arrows refer to the magnetization direction of corresponding phase.

austenite and favors the reverse martensitic phase transformation, and therefore impedes the nucleation and formation of the martensite phase. Also, the output stress induced by magnetic field acts as the energy barrier during the stress-induced martensitic transformation, and larger input power is needed to overcome the obstacle and initiate the phase transformation. (iii) For the case of our Ni-Mn-Ga-In, external magnetic field promotes the nucleation and formation of the FM martensite phase. As a sequence, the magnetic field leads to an increase in transformation temperature and a reduction in stress to trigger the martensitic transformation. From above, although the magnetostress in both Ni-Mn-Ga-In and Ni-Co-Mn-In originates from the Zeeman energy, the different magnetoresponsive effects make their output magnetostress opposite signs. The Curie temperature for martensite T_C^M higher than that for austenite T_C^A is the precondition for synergic-type transformation [35]. The higher T_C^M over T_C^A in our alloys should be attributed to their appropriate Mn-Mn distance in the martensite phase leading to stronger magnetic exchange interaction than that in the austenite phase, which is different from other Ni-Mn-based Heusler alloys [27,36].

In this context, $d\sigma_{\text{cr}}/dH$ as a parameter to characterize the magnetoresponsive effect is of crucial importance for manipulating the multicaloric effect. We compared $d\sigma_{\text{cr}}/dH$ for synergic-type $\text{Ni}_{57}\text{Mn}_{18}\text{Ga}_{21.45}\text{In}_{3.55}$ and nonsynergic-type $\text{Ni}_{45}\text{Co}_5\text{Mn}_{36.5}\text{In}_{13.5}$ in what follows.

Based on the Clausius-Clapeyron relation [2],

$$\Delta\varepsilon \times d\sigma_{\text{cr}} = -\rho\Delta S \times dT_{\text{tr}}, \quad (3)$$

the magnetic field dependence of critical stress can be deduced as

$$\frac{d\sigma_{\text{cr}}}{dH} = -\rho \frac{\Delta S_{\text{mul}}}{\Delta\varepsilon_{\text{tr}}} \times \frac{dT_{\text{tr}}}{dH}, \quad (4)$$

where $\Delta S_{\text{mul}}/\Delta\varepsilon_{\text{tr}}$ is the transformation strain dependence of entropy change corresponding to the multicaloric effect. For $\text{Ni}_{57}\text{Mn}_{18}\text{Ga}_{21.45}\text{In}_{3.55}$ and $\text{Ni}_{45}\text{Co}_5\text{Mn}_{36.5}\text{In}_{13.5}$, dT_{tr}/dH are 0.92 and -4.3 K T^{-1} [37], respectively. The density ρ for $\text{Ni}_{57}\text{Mn}_{18}\text{Ga}_{21.45}\text{In}_{3.55}$ and $\text{Ni}_{45}\text{Co}_5\text{Mn}_{36.5}\text{In}_{13.5}$ is 8100 and 8080 kg m^{-3} , respectively [27,38]. ΔS_{mul} can be determined from

$$\Delta S_{\text{mul}} = \frac{\Delta T_{\text{ad}}}{T} \times C_p, \quad (5)$$

where C_p is the specific heat for materials. C_p for $\text{Ni}_{57}\text{Mn}_{18}\text{Ga}_{21.45}\text{In}_{3.55}$ and $\text{Ni}_{45}\text{Co}_5\text{Mn}_{36.5}\text{In}_{13.5}$ [39] are 388 and $485 \text{ J kg}^{-1} \text{ K}^{-1}$, respectively.

For $\text{Ni}_{57}\text{Mn}_{18}\text{Ga}_{21.45}\text{In}_{3.55}$ in this work, ΔT_{ad} of -7.9 K is adopted on applying 95 MPa uniaxial stress and 5 T magnetic field at 303 K. For $\text{Ni}_{45}\text{Co}_5\text{Mn}_{36.5}\text{In}_{13.5}$, ΔT_{ad} of -2.9 K is taken at 293 K under 135 MPa stress field in Ref. [28]. Both alloys have the similar transforma-

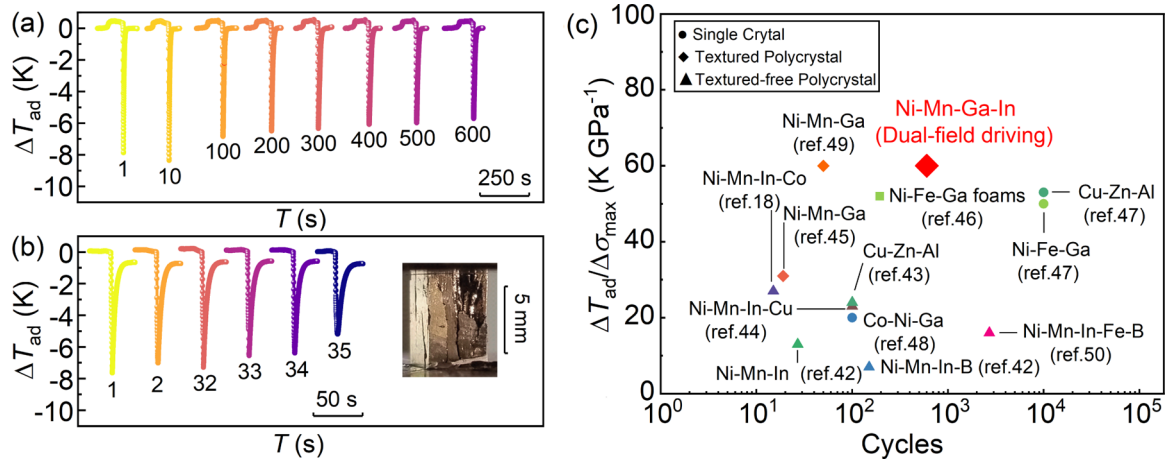


FIG. 7. ΔT_{ad} value as a function of cycle under dual fields (a) and single field (b). The inset in (b) shows the image of sample under single stress field after ~ 30 cycles. (c) Comparison of cyclic performance and $\Delta T_{ad}/\Delta\sigma_{max}$ [18,42–50].

tion strain of about 2.6%. Thus, $\Delta S_{mul}/\Delta\epsilon_{tr}$ and $d\sigma_{cr}/dH$ can be calculated as $-390 \text{ J kg}^{-1} \text{ K}^{-1}$ and -2.9 MPa T^{-1} for $\text{Ni}_{57}\text{Mn}_{18}\text{Ga}_{21.45}\text{In}_{3.55}$, and $180 \text{ J kg}^{-1} \text{ K}^{-1}$ and 6.3 MPa T^{-1} for $\text{Ni}_{45}\text{Co}_5\text{Mn}_{36.5}\text{In}_{13.5}$. The calculated data basically follow the experimental results as plotted in Fig. 6(b).

In perspective, for synergic magnetostructural transformation materials, in order to enhance magnetostress and the corresponding large multicaloric effect, stronger magnetoelastic coupling is highly desired.

C. Cyclic performance of multicaloric effect

Ni-Mn-based Heusler alloys generally suffer from the intrinsic brittleness and their cyclic performance is rather limited. Here we test the fatigue behavior for $\text{Ni}_{57}\text{Mn}_{18}\text{Ga}_{21.45}\text{In}_{3.55}$ under the dual fields of stress and magnetic field. Figure 7(a) presents ΔT_{ad} recorded during cyclic application of 95 MPa under 5 T magnetic field at 303 K for $\text{Ni}_{57}\text{Mn}_{18}\text{Ga}_{21.45}\text{In}_{3.55}$. ΔT_{ad} increases during the first few cycles, which might be attributed to the mechanical training effect [40,41]. During the subsequent 600 cycles, ΔT_{ad} degrades gradually due to the hysteresis, but still remains a relatively large value of -5.7 K . However, the alloy cracked only after about 30 cycles when subjected to the single stress cycle as seen in the inset of Fig. 7(b). Under a certain amount of transformation strain, 2.6%, as seen in Figs. 7(a) and 7(b), the ΔT_{ad} for the first cycle under pure stress field and dual fields are -7.6 and -7.9 K , respectively, which are close within the systematical errors. In terms of ΔT_{ad} , dual fields do not lead to too much improvement. On the other hand, under the constant stress of 95 MPa, an increase in ΔT_{ad} with increasing magnetic field was observed as seen in Fig. 5(c). But this increase trend of ΔT_{ad} is due to a larger transformation volume change by application of a magnetic field. As seen in Fig. 5(a), an external magnetic field of 5 T decreases σ_{cr} from 79 to 62 MPa, leading to a larger transformation strain from 1.3% to 2.6% and, consequently, an improved ΔT_{ad} from -3.9 to -7.9 K .

For practical application, a large caloric effect is not sufficient for a caloric material; some extra criteria are needed to take into consideration, such as fatigue life, $\Delta T_{ad}/\Delta\sigma_{max}$. Fatigue life is strongly related with the functional stability under

cooling cycles, while $\Delta T_{ad}/\Delta\sigma_{max}$ is usually used to evaluate the strength of a caloric effect. The larger $\Delta T_{ad}/\Delta\sigma_{max}$ is, the less input stress provided by an actuator is needed to drive a certain amount of temperature change. It is beneficial to make the cooling device more compact. Compared with other elastocaloric materials [18,42–50], $\text{Ni}_{57}\text{Mn}_{18}\text{Ga}_{21.45}\text{In}_{3.55}$ exhibits a relatively good cyclic stability under dual fields. Also, $\text{Ni}_{57}\text{Mn}_{18}\text{Ga}_{21.45}\text{In}_{3.55}$ reveals outstanding $\Delta T_{ad}/\Delta\sigma_{max}$ with value of 60 K GPa^{-1} , among other elastocaloric materials. This value could be even higher if the adiabatic condition is improved. Such a significant improvement in cyclic performance and strength of caloric effect originates from the lowered critical stress under a bias magnetic field. This indicates that for synergic-type materials, the dual-field application provides a feasible routine to lower critical stress.

IV. CONCLUSION

In this work, by tailoring the In content in $\text{Ni}_{57}\text{Mn}_{18}\text{Ga}_{25-x}\text{In}_x$ ($x = 3.4\text{--}4.3$), synergic magnetostructural transformations are achieved for alloys $x < 3.9$. Taking synergic-type $\text{Ni}_{57}\text{Mn}_{18}\text{Ga}_{21.45}\text{In}_{3.55}$ as an example, the multicaloric effect has been investigated using a bespoke multicaloric effect characterization equipment that works under uniaxial stress and magnetic field. It is found that the critical stress to trigger the transformation could be reduced by an additional magnetic field for our alloy, in contrast to nonsynergic transformation Ni-Mn-based Heusler alloys. Such a synergic feature brings about an enhancement of multicaloric adiabatic temperature change by 73% under a magnetic field of 2 T. In addition, dual-field application for $\text{Ni}_{57}\text{Mn}_{18}\text{Ga}_{21.45}\text{In}_{3.55}$ can improve the fatigue resistance compared to subjected to sole uniaxial stress.

Our work has experimentally indicated that multicaloric effect based on synergic magnetostructural transformation is a feasible strategy to achieve lower driven fields, larger transformation volume fraction, and enhanced caloric effect. However, materials exhibiting a synergic magnetostructural transformation are still somewhat scarce. It is important to develop materials showing synergic magnetostructural with strong coupling between magnetic and structural transformation. The sensitivity of critical stress to magnetic field is an

important parameter to assess the spin-lattice couple and a large positive value of magnetostress is essential for improving multicaloric effect.

ACKNOWLEDGMENTS

This research leading to these results has received funding from Zhejiang Provincial Natural Science Foundation of

China (Grant No. LD21E010001), Ningbo Science and Technology Innovation 2025 Major Project (Grant No. 2020Z063), the International Partnership Program of Chinese Academy of Sciences (Grant No. 174433KYSB20180040), and the National Natural Science Foundation of China (Grants No. 51971232 and No. 51801225). We would like to thank Dr. S. Qian from Xi'an Jiaotong University for calculation of the coefficient of performance.

-
- [1] I. Takeuchi and K. Sandeman, Solid-state cooling with caloric materials, *Phys. Today* **68**(12), 48 (2015).
- [2] X. Moya, S. Kar-Narayan, and N. D. Mathur, Caloric materials near ferroic phase transitions, *Nat. Mater.* **13**, 439 (2014).
- [3] V. Franco, J. S. Blázquez, J. J. Ipus, J. Y. Law, L. M. Moreno-Ramírez, and A. Conde, Magnetocaloric effect: From materials research to refrigeration devices, *Prog. Mater. Sci.* **93**, 112 (2018).
- [4] L. Mañosa and A. Planes, Materials with giant mechanocaloric effects: Cooling by strength, *Adv. Mater.* **29**, 1603607 (2017).
- [5] A. S. Mischenko, Q. Zhang, J. F. Scott, R. W. Whatmore, and N. D. Mathur, Giant electrocaloric effect in thin-film $\text{PbZr}_{0.95}\text{Ti}_{0.05}\text{O}_3$, *Science* **311**, 1270 (2006).
- [6] T. Gottschall, T. Gottschall, K. P. Skokov, M. Fries, A. Taubel, and O. Gutfleisch, Making a cool choice: The materials library of magnetic refrigeration, *Adv. Energy Mater.* **9**, 1901322 (2019).
- [7] L. Mañosa and A. Planes, Solid-state cooling by stress: A perspective, *Appl. Phys. Lett.* **116**, 050501 (2020).
- [8] H. L. Hou, S. X. Qian and I. Takeuchi, Materials, physics and systems for multicaloric cooling, *Nat. Rev. Mater.* (2022), doi: 10.1038/s41578-022-00428-x.
- [9] A. Planes, E. Stern-Taulats, T. Castán, E. Vives, L. Mañosa, and A. Saxena, Caloric and multicaloric effects in shape memory alloys, *Mater. Today: Proc.* **2**, S477 (2015).
- [10] Y. Liu, L. Phillips, R. Mattana, M. Bibes, A. Barthélémy, and B. Dkhil, Large reversible caloric effect in FeRh thin films via a dual-stimulus multicaloric cycle, *Nat. Commun.* **7**, 11614 (2016).
- [11] E. Stern-Taulats, T. Castán, A. Planes, L. H. Lewis, R. Barua, S. Pramanick, S. Majumdar, and L. Mañosa, Giant multicaloric response of bulk $\text{Fe}_{49}\text{Rh}_{51}$, *Phys. Rev. B* **95**, 104424 (2017).
- [12] F. X. Liang, J. Z. Hao, F. R. Shen, H. B. Zhou, J. Wang, F. X. Hu, J. He, J. R. Sun, and B. G. Shen, Experimental study on coupled caloric effect driven by dual fields in metamagnetic Heusler alloy $\text{Ni}_{50}\text{Mn}_{35}\text{In}$, *APL Mater.* **7**, 051102 (2019).
- [13] J. Liu, T. Gottschall, K. P. Skokov, J. D. Moore, and O. Gutfleisch, Giant magnetocaloric effect driven by structural transformations, *Nat. Mater.* **11**, 620 (2012).
- [14] E. Stern-Taulats, T. Castán, L. Mañosa, A. Planes, N. Mathur, and X. Moya, Multicaloric materials and effects, *MRS Bull.* **43**, 295 (2018).
- [15] Z. Wei, Y. Shen, Z. Zhang, J. Guo, B. Li, E. Liu, Z. Zhang, and J. Liu, Low-pressure-induced giant barocaloric effect in an all-d-metal Heusler $\text{Ni}_{35.5}\text{Co}_{14.5}\text{Mn}_{35}\text{Ti}_{15}$ magnetic shape memory alloy, *APL Mater.* **8**, 051101 (2020).
- [16] L. F. Zhang, J. M. Wang, H. Hua, C. B. Jiang, and H. B. Xu, Tailoring the magnetostructural transition and magnetocaloric properties around room temperature In-doped Ni-Mn-Ga alloys, *Appl. Phys. Lett.* **105**, 112402 (2014).
- [17] D. W. Zhao, T. Castán, A. Planes, Z. B. Li, W. Sun, and J. Liu, Enhanced caloric effect induced by magnetoelastic coupling in NiMnGaCu Heusler alloys: Experimental study and theoretical analysis, *Phys. Rev. B* **96**, 224105 (2017).
- [18] B. F. Lu and J. Liu, Elastocaloric effect in $\text{Ni}_{45}\text{Mn}_{36.4}\text{In}_{13.6}\text{Co}_5$ metamagnetic shape memory alloys under mechanical cycling, *Mater. Lett.* **148**, 110 (2015).
- [19] W. Sun, J. Liu, B. F. Lu, Y. Li, and A. R. Yan, Large elastocaloric effect at small transformation strain in $\text{Ni}_{45}\text{Mn}_{44}\text{Sn}$ metamagnetic shape memory alloys, *Scr. Mater.* **114**, 1 (2016).
- [20] Y. J. Huang, Q. D. Hu, N. M. Bruno, J. H. Chen, I. Karaman, Joseph H. Ross Jr., and J. G. Li, Giant elastocaloric effect in directionally solidified Ni-Mn-In magnetic shape memory alloy, *Scr. Mater.* **105**, 42 (2015).
- [21] Y. H. Qu, D. Y. Cong, S. H. Li, W. Y. Gui, Z. H. Nie, M. H. Zhang, Y. Ren, and Y. D. Wang, Simultaneously achieved large reversible elastocaloric and magnetocaloric effects and their coupling in a magnetic shape memory alloy, *Acta Mater.* **151**, 41 (2018).
- [22] T. Gottschall, A. Gràcia-Condal, M. Fries, A. Taubel, L. Pfeuffer, L. Mañosa, A. Planes, K. P. Skokov, and O. Gutfleisch, A multicaloric cooling cycle that exploits thermal hysteresis, *Nat. Mater.* **17**, 929 (2018).
- [23] J. Du, Q. Zheng, W. J. Ren, W. J. Feng, X. G. Liu, and Z. D. Zhang, Magnetocaloric effect and magnetic-field-induced shape recovery effect at room temperature in ferromagnetic Heusler alloy Ni-Mn-Sb, *J. Phys. D: Appl. Phys.* **40**, 5523 (2007).
- [24] Z. Y. Wei, W. Sun, Q. Shen, Y. Shen, Y. F. Zhang, E. K. Liu, and J. Liu, Elastocaloric effect of all-d-metal Heusler NiMnTi(Co) magnetic shape memory alloys by digital image correlation and infrared thermography, *Appl. Phys. Lett.* **114**, 101903 (2019).
- [25] T. Gottschall, K. P. Skokov, D. Benke, M. E. Gruner, and O. Gutfleisch, Contradictory role of the magnetic contribution in inverse magnetocaloric Heusler materials, *Phys. Rev. B* **93**, 184431 (2016).
- [26] P. O. Castillo-Villa, D. E. Soto-Parra, J. A. Matutes-Aquino, and R. A. Ochoa-Gamboa, Caloric effects induced by magnetic and mechanical fields in a $\text{Ni}_{50}\text{Mn}_{25-x}\text{Ga}_{25}\text{Co}_x$ magnetic shape memory alloy, *Phys. Rev. B* **83**, 174109 (2011).
- [27] J. Liu, J. Wang, L. Zhang, W. Xiao, H. Hui, and C. Jiang, Effect of isoelectronic substitution on phase transformation and magnetic properties of $\text{Ni}_{57}\text{Mn}_{18}\text{Ga}_{25-x}\text{In}_x$ ($0 \leq x \leq 8$) alloys with Ni excess, *J. Appl. Phys.* **117**, 153904 (2015).
- [28] F. B. Lu and J. Liu, Elastocaloric effect and superelastic stability in Ni-Mn-In-Co polycrystalline Heusler alloys: Hysteresis and strain-rate effects, *Sci. Rep.* **7**, 2084 (2017).

- [29] H. Hou, E. Simsek, T. Ma, N. S. Johnson, S. Qian, C. Cissé, D. Stasak, N. A. Hasan, L. Zhou, Y. Hwang, R. Radermacher, V. I. Levitas, M. J. Kramer, M. A. Zaeem, A. P. Stebner, R. T. Ott, J. Cui, and I. Takeuchi, Fatigue-resistant high-performance elastocaloric materials made by additive manufacturing, *Science* **366**, 1116 (2019).
- [30] S. Qian, J. Ling, Y. Hwang, R. Radermacher, and I. Takeuchi, Thermodynamics cycle analysis and numerical modeling of thermoelastic cooling systems, *Int. J. Refrig.* **56**, 65 (2015).
- [31] Y. Li, D. Zhao, and J. Giant and reversible room-temperature elastocaloric effect in a singlecrystalline Ni-Fe-Ga magnetic shape memory alloy, *Sci. Rep.* **6**, 25500 (2016).
- [32] H. E. Karaca, I. Karaman, B. Basaran, Y. I. Chumlyakov, and H. J. Maier, Magnetic field and stress induced martensite reorientation in NiMnGa ferromagnetic shape memory alloy single crystals, *Acta Mater.* **54**, 233 (2016).
- [33] A. S. Turabi, H. E. Karaca, H. Tobe, B. Basaran, Y. Aydogdu, and Y. I. Chumlyakov, Shape memory effect and superelasticity of NiMnCoIn metamagnetic shape memory alloys under high magnetic field, *Scr. Mater.* **111**, 110 (2016).
- [34] H. E. Karaca, I. Karaman, B. Basaran, Y. Ren, Y. I. Chumlyakov, and H. J. Maier, Magnetic field-induced phase transformation in NiMnCoIn magnetic shape-memory alloys-A new actuation mechanism with large work output, *Adv. Funct. Mater.* **19**, 983 (2009).
- [35] E. Liu, W. Wang, L. Feng, W. Zhu, G. Li, J. Chen, H. i Zhang, G. Wu, C. Jiang, H. Xu, and F. D. Boer, Stable magnetostructural coupling with tunable magnetoresponsive effects in hexagonal ferromagnets, *Nat. Commun.* **3**, 873 (2012).
- [36] P. Lázpita, J. M. Barandiarán, J. Gutiérrez, J. Feuchtwanger, V. A. Chernenko, and M. L. Richard, Magnetic moment and chemical order in off-stoichiometric Ni-Mn-Ga ferromagnetic shape memory alloys, *New J. Phys.* **13**, 033039 (2011).
- [37] R. Kainuma, Y. Imano, W. Ito, Y. Sutou, H. Morito, S. Okamoto, O. Kitakami, K. Oikawa, A. Fujita, T. Kanomata, and K. Ishida, Magnetic-field-induced shape recovery by reverse phase transformation, *Nature (London)* **439**, 957 (2006).
- [38] Ni₄₅Co₅Mn_{36.6}In_{13.4}, austenite phase (Mn1.5Co0.36Ni1.64In0.5) Crystal Structure: Datasheet from “PAULING FILE Multinaries Edition - 2012” in SpringerMaterials https://materials.springer.com/isp/crystallographic/docs/sd_1819705.
- [39] T. Kihara, X. Xu, W. Ito, R. Kainuma, and M. Tokunaga, Direct measurements of inverse magnetocaloric effects in metamagnetic shape-memory alloy NiCoMnIn, *Phys. Rev. B* **90**, 214409 (2014).
- [40] K. Engelbrecht, J. Tušek, S. Sanna, D. Eriksen, O. V. Mishin, C. R. H. Bahl, and N. Pryds, Effects of surface finish and mechanical training on Ni-Ti sheets for elastocaloric cooling, *APL Mater.* **4**, 064110 (2016).
- [41] Q. Shen, D. Zhao, W. Sun, Z. Wei, and J. liu, Microstructure, martensitic transformation and elastocaloric effect in Pd-In-Fe polycrystalline shape memory alloys, *Intermetallics* **100**, 27 (2018).
- [42] Z. Yang, D. Y. Cong, X. M. Sun, Z. H. Nie, and Y. D. Wang, Enhanced cyclability of elastocaloric effect in boron-microalloyed Ni-Mn-In magnetic shape memory alloys, *Acta Mater.* **127**, 33 (2017).
- [43] L. Mañosa, S. Jarque-Farnos, E. Vives, and A. Planes, Large temperature span and giant refrigerant capacity in elastocaloric Cu-Zn-Al shape memory alloys, *Appl. Phys. Lett.* **103**, 211904 (2013).
- [44] X. Tang, Y. Feng, H. Wang, and P. Wang, Enhanced elastocaloric effect and cycle stability in B and Cu co-doping Ni-Mn-In polycrystals, *Appl. Phys. Lett.* **114**, 1 (2019).
- [45] D. Li, Z. B. Li, J. J. Yang, Z. Z. Li, B. Yang, H. L. Yan, D. H. Wang, L. Hou, X. Li, Y. D. Zhang, C. Esling, X. Zhao, and L. Zuo, Large elastocaloric effect driven by stress-induced two-step structural transformation in a directionally solidified Ni₅₅Mn₁₈Ga alloy, *Scr. Mater.* **163**, 116 (2019).
- [46] M. Imran and X. Zhang, Elastocaloric effects in polycrystalline Ni-Fe-Ga foams with hierarchical pore architecture, *Phys. Rev. Materials* **4**, 065403 (2020).
- [47] Y. Wu, E. Ertekin, and H. Sehitoglu, Elastocaloric cooling capacity of shape memory alloys – Role of deformation temperatures, mechanical cycling, stress hysteresis and inhomogeneity of transformation, *Acta Mater.* **135**, 158 (2017).
- [48] A. Shen, D. W. Zhao, W. Sun, J. Liu, and C. J. Li, Elastocaloric effect in a Co₅₀Ni₂₀Ga single crystal, *Scr. Mater.* **127**, 1 (2017).
- [49] L. Wei, X. X. Zhang, J. Liu, and L. Geng, Orientation dependent cyclic stability of the elastocaloric effect in textured Ni-Mn-Ga alloys, *AIP Adv.* **8**, 055312 (2018).
- [50] Z. Yang, D. Y. Cong, Y. Yuan, Y. Wu, Z. H. Nie, R. G. Li, and Y. D. Wang, Ultrahigh cyclability of a large elastocaloric effect in multiferroic phase-transforming materials, *Mater. Res. Lett.* **7**, 137 (2019).